© 2019. Published by The Company of Biologists Ltd | Journal of Cell Science (2019) 132, jcs231720. doi:10.1242/jcs.231720

RESEARCH ARTICLE

The cytoplasmic C-terminal region of the ATP11C variant determines its localization at the polarized plasma membrane

Masahiro Takayama*, Hiroyuki Takatsu*, Asuka Hamamoto, Hiroki Inoue, Tomoki Naito‡, Kazuhisa Nakayama and Hye-Won Shin§

ABSTRACT

ATP11C, a member of the P4-ATPase family, is a major phosphatidylserine (PS)-flippase located at the plasma membrane. ATP11C deficiency causes a defect in B-cell maturation, anemia and hyperbilirubinemia. Although there are several alternatively spliced variants derived from the *ATP11C* gene, the functional differences between them have not been considered. Here, we compared and characterized three C-terminal spliced forms (we designated as ATP11C-a, ATP11C-b and ATP11C-c), with respect to their expression patterns in cell types and tissues, and their subcellular localizations. We had previously shown that the C-terminus of ATP11C-a is critical for endocytosis upon PKC activation. Here, we found that ATP11C-b and ATP11C-c did not undergo endocytosis upon PKC activation. Importantly, we also found that ATP11C-b localized to a limited region of the plasma membrane in polarized cells, whereas ATP11C-a was distributed on the entire plasma membrane in both polarized and non-polarized cells. Moreover, we successfully identified LLXY residues within the ATP11C-b C-terminus as a critical motif for the polarized localization. These results suggest that the ATP11C-b regulates PS distribution in distinct regions of the plasma membrane in polarized cells.

KEY WORDS: Cell polarity, Membrane lipids, Transporters, Flippase, P4-ATPase, P-type ATPase

INTRODUCTION

Lipid bilayers of cellular membranes exhibit asymmetric lipid distributions. In mammalian cells, the aminophospholipids phosphatidylserine (PS) and phosphatidylethanolamine (PE) are abundant in the cytoplasmic leaflet, whereas phosphatidylcholine (PC) and sphingomyelin are enriched in the exoplasmic leaflet of the plasma membrane (Devaux, 1991; Murate et al., 2015; Zachowski, 1993). PS is abundant on the cytoplasmic side of both the plasma membrane and recycling endosomes (Fairn et al., 2011; Tanaka et al., 2016; Uchida et al., 2011), and plays important roles in recruiting and/or activating regulatory proteins, such as protein kinase C (PKC), K-Ras, Cdc42, Rac1 and EHD1, and thus affects signal transduction, cell polarity, cell migration and membrane trafficking (Das et al., 2012; Finkielstein et al., 2006; Lee et al., 2015; Tanaka et al., 2016; Yeung et al., 2009). Since P4-ATPases translocate aminophospholipids from the exoplasmic (or luminal) to the cytoplasmic leaflets of cellular membranes (Andersen et al., 2016; Takatsu et al., 2014), the presence of P4-ATPases in the plasma membrane and cellular organelles (Takatsu et al., 2011) underlies the asymmetric distribution of phospholipids in these membranes.

Among human P4-ATPases, ATP11A and ATP11C localize to the plasma membrane and flip nitrobenzoxadiazole (NBD)-labeled PS (NBD–PS) and NBD–PE, whereas ATP8B1, ATP8B2 and ATP10A flip NBD–PC specifically at the plasma membrane (Naito et al., 2015; Shin and Takatsu, 2019; Takada et al., 2015; Takatsu et al., 2014). Moreover, we recently found that ATP10D flips NBD–glucosylceramide specifically, but not phospholipids, at the plasma membrane (Roland et al., 2019). These P4-ATPases interact with CDC50A, which is required for their transport from the endoplasmic reticulum to the plasma membrane in HeLa cells (Naito et al., 2015; Shin and Takatsu, 2019; Takatsu et al., 2011). Among P4-ATPase family members, ATP11C is relatively well studied with respect to its cellular functions. ATP11C and ATP11A are irreversibly downregulated during apoptosis via caspase-mediated cleavage (Segawa et al., 2014). Moreover, ATP11C is reversibly downregulated by Ca^{2+}-dependent PKC activation in living cells (Takatsu et al., 2017). ATP11C is a major PS-flippase in certain cell types, such as CHO-K1 and KBM-7 cells, leukocytes, bone marrow B cells and erythrocytes (Arashiki et al., 2016; Segawa et al., 2014, 2018; Takada et al., 2015; Yabas et al., 2016). In addition, ATP11C is highly expressed in rat liver, especially basolateral membranes of hepatocytes (Chaubey et al., 2016). Indeed, ATP11C deficiency causes a defect in B-cell maturation, altered erythrocyte shape, anemia and hyperbilirubinemia (Siggs et al., 2011b; Yabas et al., 2014, 2011).

There are two N-terminal and three C-terminal splice variants in human *ATP11C*, while only three C-terminal splice variants are found in mouse *Atp11c*. Although the function and expression of ATP11C has been relatively well-studied in various cell types and tissues, as described above, the differences between these variants have not been explored. ATP11C-a possesses a di-leucine-like motif (SVRPLL) in its C-terminal cytoplasmic region and can undergo endocytosis soon after PKCα phosphorylates the Ser residue (Takatsu et al., 2017).

In the present study, we focused on the three ATP11C C-terminal splice variants, designated as ATP11C-a, ATP11C-b and ATP11C-c, which are found in both humans and mice, and compared their expression and subcellular localization. We showed that unlike ATP11C-a, neither ATP11C-b nor ATP11C-c harbors an endocytic motif, and hence they do not undergo PKC-mediated endocytosis. Importantly, we found that ATP11C-b localizes to a confined area at the plasma membrane in polarized cells. We further characterize the LLXYKH residues found in ATP11C-b as the motif responsible for its polarized localization. Thus, this motif may enable the specific functions of ATP11C-b in polarized cells.

Department of Physiological Chemistry, Graduate School of Pharmaceutical Sciences, Kyoto University, Sakyo-ku, Kyoto 606-8501, Japan.
*These authors contributed equally to this work
‡Present address: Lee Kong Chian School of Medicine, Nanyang Technological University, 11 Mandalay Road, 308232, Singapore.

§Author for correspondence (shin@pharm.kyoto-u.ac.jp)

H.-W.S., 0000-0002-9138-9554

Received 10 March 2019; Accepted 22 July 2019

Journal of Cell Science (2019) 132, jcs231720. doi:10.1242/jcs.231720

RESULTS

The expression level of C-terminal variants of ATP11C varies depending on the cell type and tissue

There are three C-terminal splice variants of mouse Atp11c, whereas five isoforms of human ATP11C generated via a combination of two N-terminal and three C-terminal splice variations are listed in public databases (Fig. S1). We first examined the expression levels of three C-terminal splice variants in a variety of cell types and various mouse tissues through RT-PCR. Because all of the three C-terminal variants of mouse and human include exon 31 (Fig. 1A), although they are generated via alternative splicing, the mRNA levels of the three variants can be directly compared using the same primer set as shown in Fig. 1A. Overall, although proportions of the expression levels of ATP11C-a, ATP11C-b and ATP11C-c varied in different cell types and tissues, ATP11C-a and ATP11C-b were expressed in most cell types and tissues (Fig. 1B,C). ATP11C-c had a limited expression pattern, with the highest levels found in the brain (Fig. 1B). ATP11C-b was predominantly expressed in mouse bone marrow, heart and spleen, while ATP11C-a was hardly expressed in bone marrow and spleen, in which blood cells are enriched. Notably, ATP11C-b was predominantly expressed in the highly invasive breast cancer cell line MDA-MB-231, but was hardly expressed in non-invasive breast cancer cell lines MCF-7 and MDA-MB-453 (Fig. 1C). ATP11C-b was predominantly expressed in motile leukocytes (KBM7, Raw264.7, Ba/F3 and W3 cells) and RPE-1 cells. We sequenced some of the PCR products (from mouse brain, liver, HeLa and 293T) and confirmed the isoform types. We also analyzed expression of isoforms in mouse tissues and human cell lines with real-time quantitative RT-PCR (qRT-PCR) (Fig. S2). Both ATP11C-a and ATP11C-b showed the highest expression levels in liver, and ATP11C-b, but not ATP11C-a, was highly expressed in bone marrow. Consistent with the data shown in Fig. 1C, the qRT-PCR analysis demonstrated that ATP11C-b is expressed at a relatively high level in MDA-MB-231 cells, but at a low level in MCF-7 cells (Fig. S2).

Comparative analyses of the subcellular localizations of C-terminal splice variants of ATP11C upon PMA treatment

We have previously shown that the C-terminal cytoplasmic region of ATP11C-a (Fig. 2A) is critical for Ca^{2+} signaling-dependent

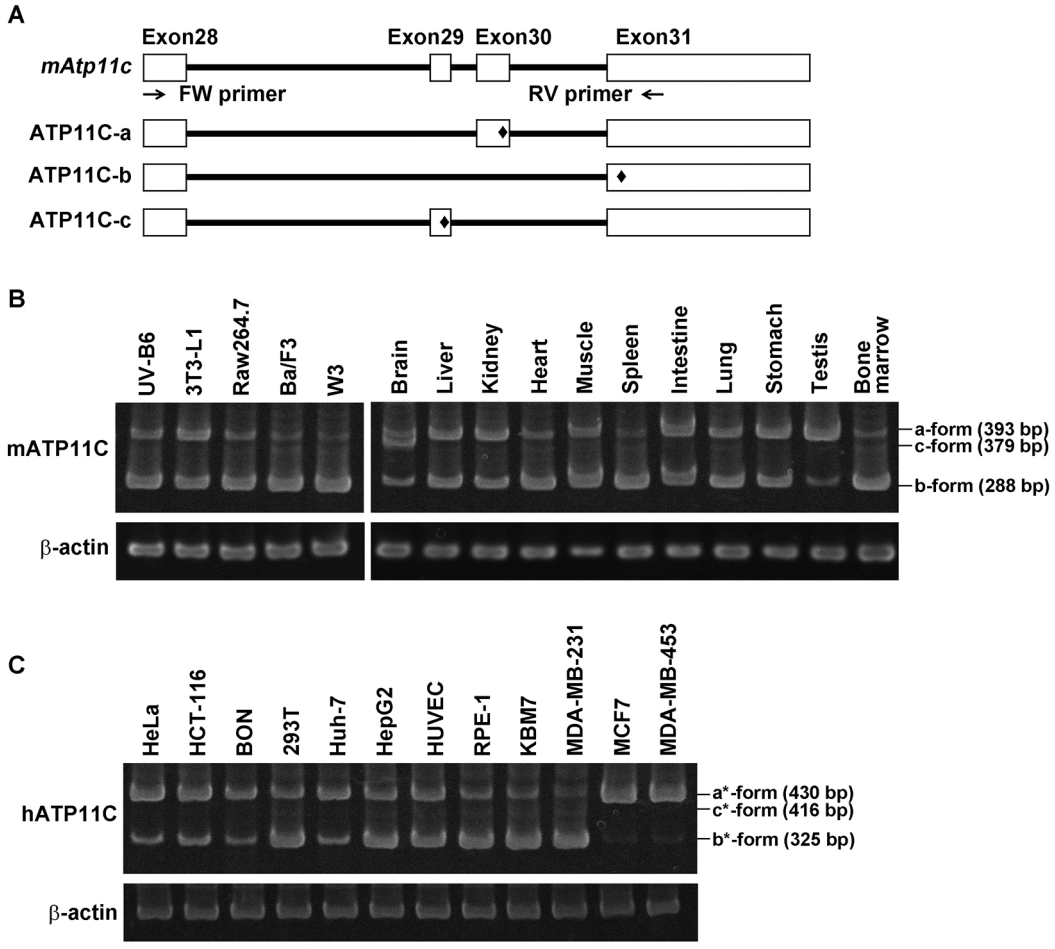

Fig. 1. Expression level of C-terminal isoforms of ATP11C. (A) Part of the mouse *Atp11c* gene, which has the same structure as human *ATP11C*. Schematic representation of the three C-terminal splicing variants in mouse and human ATP11C. The primer set for amplifying three variants simultaneously is indicated (FW, forward and RV, reverse). ♦ indicates a stop codon. (B,C) RT-PCR was performed using total RNA isolated from each cell and mouse tissue. The product sizes of mouse ATP11C-a, ATP11C-b and ATP11C-c are 393, 288 and 379 base pairs, respectively (B); those of human ATP11C-a*, ATP11C-b* and ATP11C-c* (see Fig. S1) are 430, 325 and 416 base pairs, respectively (C). * indicates mixture of two N-terminal splice forms of human ATP11C. The PCR products were subjected to 5% PAGE to discriminate a-form and c-form sizes. UV-B6, transformed skin fibroblasts; 3T3-L1, fibroblasts; Raw264.7, transformed macrophages; Ba/F3, ProB cells; W3, transformed T-cell lymphoma cells; HeLa, cervical carcinoma cells; HCT-116, colorectal carcinoma cells; BON, neuroendocrine cancer cells; 293T, transformed embryonic kidney cells; Huh-7 and HepG2, hepatoma cells; HUVEC, umbilical vein endothelial cells; RPE-1, transformed retinal pigment epithelial cells; KBM-7, myeloid leukemia cells; MDA-MB-231, invasive breast cancer cells; MCF-7 and MDA-MB-453, non-invasive breast cancer cells.

Journal of Cell Science (2019) 132, jcs231720. doi:10.1242/jcs.231720

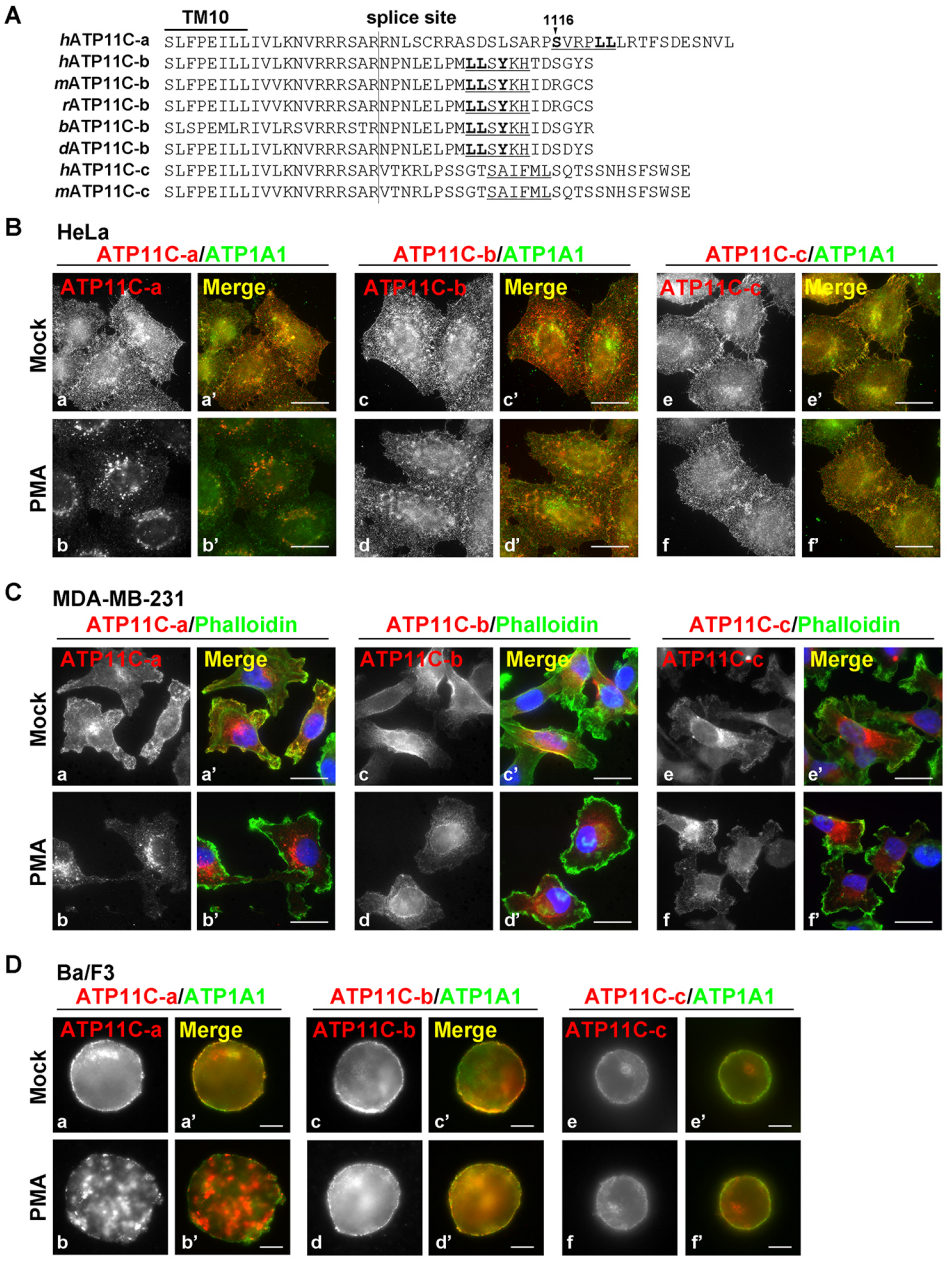

Fig. 2. Subcellular localization of the C-terminal splice variants of ATP11C. (A) Alignment of amino acid sequences of the C-terminal cytoplasmic region of mammalian variants of ATP11C. The ATP11C-a sequence shown in bold is involved in endocytosis of ATP11C upon PKC activation. The underlined LLSYKH residues are conserved among human (*h*), mouse (*m*), rat (*r*), bovine (*b*) and dog (*d*). In particular, residues LLXY, in bold, are critical residues for polarized localization of ATP11C-b (see Figs 6 and 8). (B–D) HeLa, MDA-MB-231 and Ba/F3 cells stably expressing C-terminally HA-tagged ATP11C-a, ATP11C-b and ATP11C-c (we here used a construct including the same N-terminus as ATP11C-a and -b) were treated for 15 min at 37°C with vehicle alone (Mock) or with 400 nM of PMA (PMA). The cells were fixed and immunostained with anti-HA (3F10) alone or anti-HA and anti-ATP1A1 (marker for the plasma membrane) antibodies, followed by Cy3-conjugated anti-rat-IgG and Alexa Fluor 488-conjugated phalloidin or Alexa Fluor 488-conjugated anti-rabbit-IgG secondary antibodies. Scale bars: 20 µm (B,C) and 5 µm (D).

endocytosis (Takatsu et al., 2017). We therefore hypothesized that the C-terminal region of ATP11C is important for regulation of its cellular function. To compare the cellular localization of the three C-terminal variants, we established cells stably expressing C-terminally HA-tagged ATP11C-a, ATP11C-b or ATP11C-c in HeLa, MDA-MB-231 and Ba/F3 cells (Takatsu et al., 2014) (Fig. 2). The SXXXLL motif in ATP11C-a acts as a di-leucine motif (D/EXXXLL) when the serine residue (S1116) is phosphorylated (pSXXXLL) via Ca^{2+}-dependent PKCα activation (Takatsu et al., 2017) (Fig. 2A). The di-leucine motif plays a key role as an endocytic sorting signal by interacting with the clathrin adaptor protein complex (Bonifacino and Traub, 2003; Kelly et al., 2008). The C-terminal region of ATP11C-b is well conserved in mammals, but does not harbor a di-leucine-like motif (Fig. 2A). Upon PMA treatment, ATP11C-a was endocytosed in HeLa, MDA-MB-231 and Ba/F3 cells as shown previously (Fig. 2B–D, panels labeled b and b′) (Takatsu et al., 2017). By contrast, ATP11C-b was retained at the plasma membrane upon PMA treatment (Fig. 2B–D, panels labeled d and d′). ATP11C-c includes a conserved SAIFML sequence resembling the SXXXLL motif (Fig. 2A), but it did not undergo endocytosis upon PMA treatment (Fig. 2B–D, panels labeled f and f′), suggesting the sequence does not serve as an endocytic signal upon PKC activation.

In the course of the experiment, we unexpectedly found that ATP11C-b localized to a confined area of the plasma membrane and was excluded from the peripheral lamellipodia in polarized MDA-MB-231 cells (Fig. 2C, panels labeled c and c′), although the ATP11C variant was uniformly distributed on the plasma membrane in non-polarized HeLa and Ba/F3 cells (Fig. 2B,D, panels labeled c and c′). By contrast, ATP11C-a and ATP11C-c were found on the entire plasma membrane in both polarized and non-polarized cells (Fig. 2B–D, panels labeled a, a′, e, and e′). Therefore, we hereafter focused on the ATP11C-b variant together with ATP11C-a; both variants are ubiquitously expressed (Fig. 1).

Journal of Cell Science (2019) 132, jcs231720. doi:10.1242/jcs.231720

We determined relative cell-surface expression levels of ATP11C-a and ATP11C-b upon PMA treatment by surface biotinylation and following quantification of the band intensities of the biotinylated proteins. Upon PMA treatment, the cell surface level of ATP11C-a decreased, as previously described (Takatsu et al., 2017) (Fig. 3A,B). By contrast, the level of ATP11C-b on the cell surface did not decrease, but rather increased, upon PMA treatment (Fig. 3A,B). Therefore, only the ATP11C-a variant is downregulated via signal-dependent PKC activation.

We examined the flippase activity of cells expressing ATP11C-a and ATP11C-b upon PMA treatment. ATP11C-a was previously shown to translocate PS and PE at the plasma membrane (Takatsu et al., 2011, 2014). When stably expressed in Ba/F3 cells, ATP11C-a and ATP11C-b translocated NBD-labeled PS (NBD-PS) and NBD-PE to a similar extent (Fig. 3C). The PS- and PE-flippase activities in cells expressing ATP11C-b did not decrease upon PMA treatment, whereas the activities decreased dramatically in cells expressing ATP11C-a (Fig. 3C) (Takatsu et al., 2017). Therefore, the decrease in the PS/PE-flippase activity at the plasma membrane can be attributed to sequestration of ATP11C-a from the plasma membrane (Takatsu et al., 2017). The basal PS-flippase activity in parental Ba/F3 cells (–) also decreased upon PMA treatment, probably due to downregulation of endogenous ATP11C-a (Fig. 3C).

ATP11C-b localizes to the uropod specifically whereas ATP11C-a is uniformly distributed on the plasma membrane in polarized Ba/F3 cells

In the course of our experiments, we recognized that Ba/F3 (proB) cells are highly motile and polarized (cells have a distinct anterior and posterior) in normal growth medium, but they readily rounded up and lost polarity following subtle stress, such as pipetting, medium changes or pelleting via centrifugation (Fig. 2D). To preserve the polarized phenotype of Ba/F3 cells during immunofluorescence analysis, we added paraformaldehyde (PFA) solution directly into the growth medium to fix the Ba/F3 cells immediately. The immediate fixation made it easy to observe the polarized Ba/F3 cells by immunofluorescence analysis. Intriguingly, ATP11C-b was found to localize to a limited area of the plasma membrane in the polarized Ba/F3 cells (Fig. 4Ac,Bb,Cb,Da,Ea) even though it was uniformly distributed at the plasma membranes of non-polarized Ba/F3 (rounded) and HeLa cells (Figs 2 and 4Ad; Fig. S3). By contrast, ATP11C-a demonstrated uniform distribution on the plasma membrane in both polarized and non-polarized cells (Fig. 4Aa,Ab,Ba,Ca; Fig. S3).

Motile leukocytes exhibit a polarized morphology characterized by the formation of leading-edge pseudopods and a highly contractile cell posterior known as the uropod (Fig. 4F) (Hind et al., 2016). The nucleus is located at the cell anterior, while the microtubule-

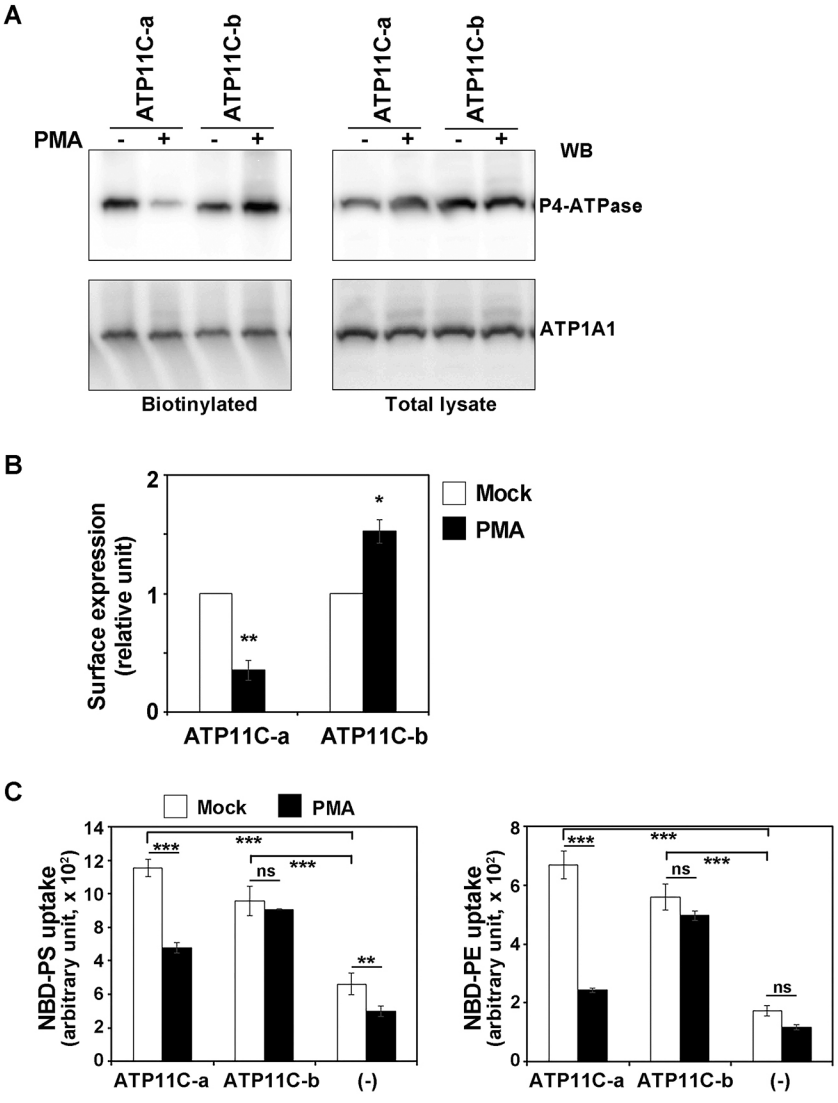

Fig. 3. ATP11C-a and ATP11C-b were differentially regulated by PKC activation. (A) Cell-surface expression levels of ATP11C-a and ATP11C-b following treatment with PMA in HeLa cells were analyzed after surface biotinylation. Proteins precipitated with streptavidin–agarose beads were subjected to immunoblot analysis (left panels, biotinylated). 10% of the input of the biotinylation reaction was loaded in each lane (right panels, total lysate). Expression of ATP11C-a and ATP11C-b proteins was analyzed by immunoblotting with anti-HA and anti-ATP1A1 (as an internal control) antibodies. (B) Relative surface expression levels of proteins normalized against the level of ATP1A1 (used as an internal control). Graphs display means±s.d. from four independent experiments. **P*<0.05, ***P*<0.001 in comparison to mock-treated cells (Student's *t*-test). (C) Ba/F3 cells stably expressing HA-tagged ATP11C-a and ATP11C-b, and parental cells (–) were treated with vehicle alone (white bars) or 400 nM PMA (black bars) for 15 min. The cells were then washed with flippase assay buffer and incubated with NBD-PS for 5 min or NBD-PE for 15 min at 15°C. After extraction with fatty acid-free BSA, the residual fluorescence intensity associated with the cells was determined via flow cytometry. Graph displays means from three independent experiments as mean±s.d. ***P*<0.001, ****P*<0.0001; ns, not significant (two-way ANOVA was used to assess variance and comparisons between data sets were made using Dunnett's analysis).

Journal of Cell Science (2019) 132, jcs231720. doi:10.1242/jcs.231720

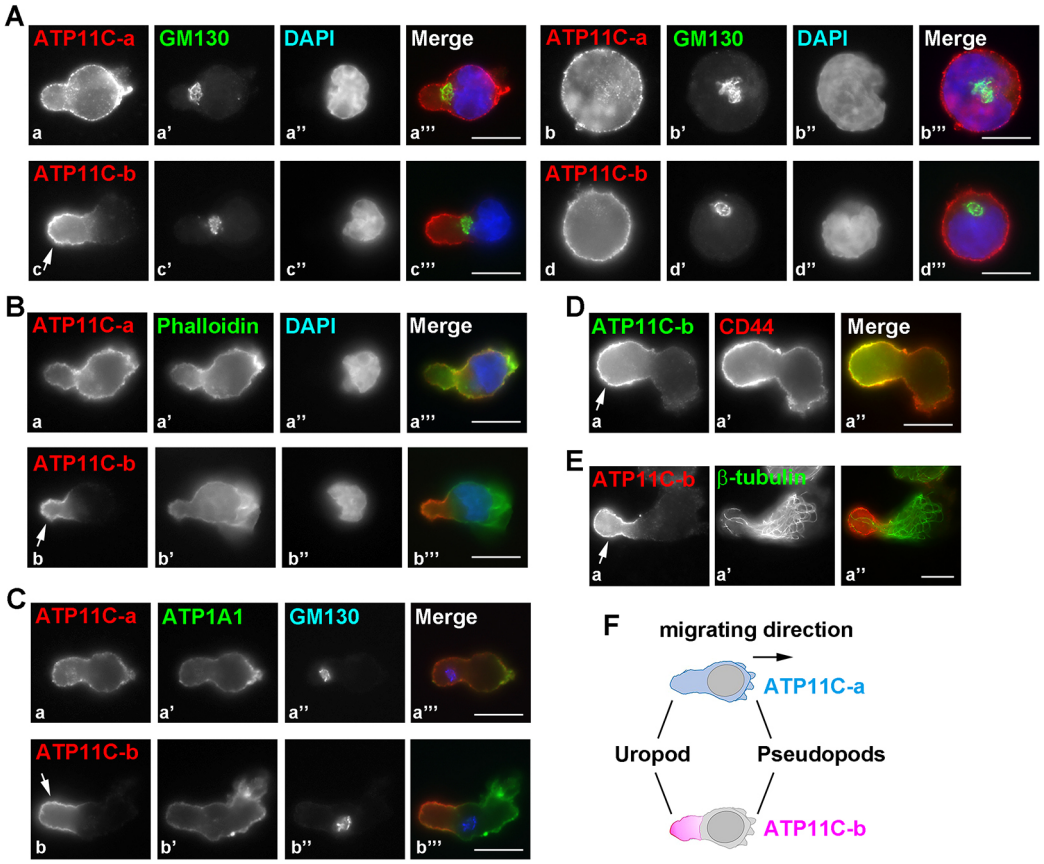

Fig. 4. ATP11C-b localized to the uropod in polarized Ba/F3 cells. (A–C) Ba/F3 cells stably expressing C-terminally HA-tagged ATP11C-a or ATP11C-b were fixed by adding PFA directly into the medium and triply stained for HA (3F10), GM130 and DAPI (A); for HA, F-actin (phalloidin) and the nucleus (DAPI) (B); or for HA, ATP1A1 and GM130 (C) followed by incubation with Cy3-conjugated anti-rat-IgG and Alexa Fluor 488-conjugated anti-rabbit-IgG or with Cy3-conjugated anti-rat-IgG, Alexa Fluor 488-conjugated anti-mouse-IgG and DyLight 649-conjugated anti-rabbit-IgG secondary antibodies. DAPI or Alexa Fluor 488-conjugated phalloidin were added with the secondary antibodies. In A, panels a–a‴ and c–c‴ show polarized BaF3 cells, and b–b‴ and d–d‴ show non-polarized Ba/F3 cells. (D) Cells were doubly stained for HA (4B2) and CD44 followed by incubation with Alexa Fluor 488-conjugated anti-mouse-IgG and Cy3-conjugated anti-rat-IgG secondary antibodies. (E) Cells were doubly stained for HA (3F10) and β-tubulin followed by incubation with Cy3-conjugated anti-rat-IgG and Alexa Fluor 488-conjugated anti-mouse-IgG secondary antibodies; here a is an image focused on the plasma membrane while a′ and a″ are focused on microtubules. Arrows in all panels highlight uropods. Scale bars: 10 µm. (F) Schematic localization of ATP11C-a in blue and ATP11C-b in pink. ATP11C-a was distributed throughout the plasma membrane, whereas ATP11C-b was confined to the uropod in polarized Ba/F3 cells.

organizing center and the Golgi complex are positioned posterior to the nucleus in migrating leukocytes (Fig. 4Aa′″,c′″) (Hind et al., 2016; Niggli, 2014; Valignat et al., 2014; Wojtal et al., 2006). ATP11C-b was confined to the plasma membrane of the cell posterior, the uropod, and excluded from the cell anterior, where the nucleus is located (Fig. 4Ac–c′″), and pseudopods, where F-actin rearrangement is active (Fig. 4Bb–b′″). As shown in Movie 1, in motile Ba/F3 cells, GFP-tagged ATP11C-b specifically localized to the uropod (cell posterior) plasma membrane, whereas GFP-tagged ATP11C-a was distributed throughout the plasma membrane. CD44 (known as a component of the uropod) is concentrated in the cell rear, where ATP11C-b is confined (Fig. 4D). ATP1A1, which is a plasma membrane marker in non-polarized cells and a basolateral membrane marker in polarized epithelial cells, appeared distributed on the entire plasma membrane with slight concentration in the cell anterior, where ATP11C-b is excluded (Fig. 4Ca′,b′; Fig. S5A). We then established Ba/F3 cells stably co-expressing EGFP–ATP11C-a and tRFP–ATP11C-b to compare distribution of ATP11C-a and ATP11C-b in living cells. As shown in Movie 2, ATP11C-b was confined to the uropod on the posterior side of migrating Ba/F3 cells, whereas ATP11C-a was found on the entire plasma membrane, including the pseudopods and uropod.

ATP11C-b is confined to the bile canalicular plasma membrane in HepG2 cells

ATP11C is expressed at the high level in the liver (Chaubey et al., 2016), and appears to be involved in transport of bile acids across the sinusoidal membrane (de Waart et al., 2016; Matsuzaka et al., 2015). Hepatocytes are polarized cells with bile canalicular and sinusoidal domains, which are equivalent to the apical and basolateral surfaces, respectively, of polarized epithelial cells (Zegers and Hoekstra, 1998). HepG2 cells are well-polarized hepatoma cells that are used as a model system for hepatocytes (Sormunen et al., 1993). Apical membranes of HepG2 cells form a closed space between adjacent cells, representing the bile canaliculus, which is identified by the presence of dense F-actin (Fig. 5A′,B′) (Wojtal et al., 2006). Since both ATP11C-a and ATP11c-b are expressed in the liver (Fig. 1C), we established HepG2 cells stably expressing N-terminally EGFP-tagged ATP11C-a or ATP11C-b and observed their localization. Intriguingly, ATP11C-b was specifically concentrated in the canalicular plasma membrane in polarized HepG2 cells, whereas ATP11C-a was distributed to the entire plasma membrane (Fig. 5), indicating that ATP11C-b was confined to the apical plasma membrane in hepatocytes.

Journal of Cell Science (2019) 132, jcs231720. doi:10.1242/jcs.231720

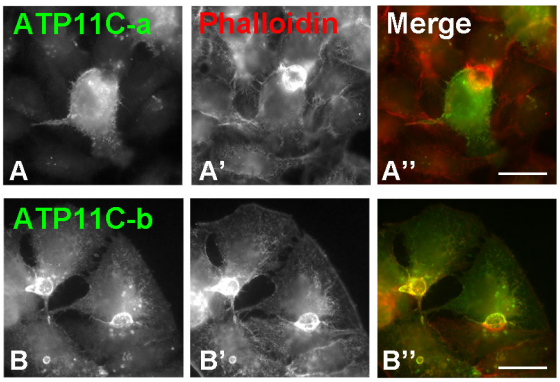

Fig. 5. Localization of ATP11C isoforms in polarized HepG2 cells. HepG2 cells stably expressing N-terminally EGFP-tagged ATP11C-a (A) or ATP11C-b (B) were fixed and incubated with Alexa Fluor 555-conjugated phalloidin. The bile canalicular plasma membrane was visualized by F-actin staining. Scale bars: 20 µm.

ATP11C-b is localized to the cell body and excluded from the lamellipodia in polarized MDA-MB-231 cells

ATP11C-b was predominantly expressed not only in Ba/F3 cells, but also in the highly invasive MDA-MB-231 cells (Fig. 1B). F-actin was extensively labeled by phalloidin at the lamellipodia, where actin rearrangement actively occurs (Fig. 6A, enlargement 1), and F-actin was also labeled at the cortex in the cell body, where rather stable actin filaments are formed (Fig. 6A, enlargement 2). As briefly described above, ATP11C-b was colocalized with F-actin in the cell body (b–b″ and enlargement 2) and absolutely excluded from the lamellipodia (b–b″ and enlargement 1). By contrast, ATP11C-a was found on the entire plasma membrane with relative concentration at the lamellipodia (Fig. 6Aa–a″, and enlargements). As shown in Movie 3, GFP-tagged ATP11C-b specifically localized to the cell body, but not to the lamellipodia, whereas GFP-tagged ATP11C-a was distributed to the entire plasma membrane, including the lamellipodia, in MDA-MB-231 cells. Taken together, ATP11C-b was not localized to areas of the plasma membrane where actin remodeling is active, such as the pseudopods and lamellipodia in Ba/F3 and MDA-MB-231 cells, respectively. By contrast, it was confined to the uropod and the cell body in Ba/F3 and MDA-MB-231 cells, respectively, in which F-actin may be more stable (Figs 4 and 6A).

The LLSYKH sequence in the ATP11C-b C-terminal region is critical for polarized localization

We hypothesized that the 20-amino-acid C-terminal region of ATP11C-b (Fig. 2A) harbors the signal for its polarized localization. To identify amino acid residues critical for polarized localization, we first divided the region into blocks of five amino acids and replaced each block individually with alanine residues, transiently co-expressed each mutant with FLAG–CDC50A in MDA-MB-231 cells and examined their localization (Fig. S4); because it was impossible to transfect plasmid DNA into Ba/F3 cells, we used MDA-MB-231 cells for the screening of the alanine mutants. Among them, the LPMLL/AAAAA and SYKHT/AAAAA mutants were found to be mislocalized to the lamellipodia. By contrast, NPLNE/AAAAA and DSGYS/AAAAA mutants were localized to the cell body, but not to the lamellipodia, like wild-type ATP11C-b (Fig. S4). These observations indicate that the amino acid residues responsible for the polarized localization ATP11C-b are included in the LPMLLSYKHT residues. We then divided this sequence into blocks of two amino acids, replaced each block individually with alanine residues, and examined localization of each mutant. Although the first LP residues appeared to be dispensable for the polarized localization, other mutations affected the polarized localization of ATP11C-b to some degree (Fig. S4). Therefore, we finally focused on eight amino acids (MLLSYKHT). To determine the contribution of individual amino acids, we generated eight different mutants, each having one of the eight amino acids replaced with an alanine residue, and examined the cellular localization of each mutant in MDA-MB-231 cells (Fig. 6B–D). The L1108A, L1109A and Y1111A mutants were mislocalized to the lamellipodia (Fig. 6Cb–b″, c–c″ and e–e″), whereas the other mutants were mainly localized to the cell body and excluded from the lamellipodia, similar to wild-type ATP11C-b (Fig. 6Ca–a″, d–d″ and f–h″). We counted the numbers of cells in which the ATP11C proteins were localized to the cell body and peripheral lamellipodia, and those in which the proteins were localized to the cell body only (Fig. 6D). ATP11C-a was distributed to the entire plasma membrane, including cell body and lamellipodia, whereas ATP11C-b localized exclusively to the cell body (Fig. 6D). Replacement of L1108, L1109 or Y1111 with an alanine residue abrogated the polarized localization of ATP11C-b, causing it to mislocalize to the lamellipodia (Fig. 6D). On the other hand, mutation of K1112 or H1113 to alanine only modestly affected the polarized localization (Fig. 6D). Taken together, the L1108, L1109 and Y1111 residues appear to be critical for the polarized localization of ATP11C-b, while the K1112 and H1113 residues may play an auxiliary role. We also established Ba/F3 cells stably expressing the single amino-acid-replacement mutants and observed the localization of each mutant protein. However, unlike localization of the point mutants in MDA-MB-231 cells, the point mutations only marginally affected the localization of ATP11C-b to the uropod in Ba/F3 cells (Fig. S5). Therefore, we next substituted six alanine residues for the LLSYKH residues (Fig. 6B), expressed the mutant ATP11C-b(6Ala) stably in Ba/F3 cells, and observed its cellular localization (Fig. 7A,B; Fig. S5). This mutation completely abolished the polarized localization of ATP11C-b in Ba/F3 cells (Fig. 7A,B, panels labeled b and c; Fig. S5). The mutant was distributed to the entire plasma membrane, including the cell anterior (pseudopods) and the uropod in polarized Ba/F3 cells (Fig. 7Ac,Bc). Therefore, LLSYKH residues are critical for ATP11C-b localization to the uropod.

Mislocalization of ATP11C-b did not significantly affect cell polarity

We next asked whether mislocalization of ATP11C-b affects cell polarity generation and maintenance. Although the polarized localization of ATP11C-b was abolished after mutating six amino acids in the C-terminal region [ATP11C-b(6Ala)] (Fig. 7A,B, panels labeled b and c), cell polarity was largely unaffected. Pseudopods were formed at the leading edge as normal (Fig. 7Aa′–c′), and the nucleus and the Golgi complex were located in the normal location in the polarized Ba/F3 cells (Fig. 7Ba′–c′ and a″–c″). We also confirmed that ATP11C-b(6Ala) appeared to be localized to the lamellipodia in addition to the cell body in MDA-MB-231 cells (Fig. 8B). Lamellipodia formation also was not significantly affected by mislocalization of ATP11C-b in MDA-MB-231 cells (Fig. 8B). These observations together indicate that mislocalization of ATP11C-b may not, at least substantially, affect the cell polarity. We next examined whether the 6Ala mutation affects the flippase activity of ATP11C-b. The expression level of ATP11C-b(6Ala) in Ba/F3 cells was comparable to that of ATP11C-b(WT) (Fig. 7C). As shown in

Journal of Cell Science (2019) 132, jcs231720. doi:10.1242/jcs.231720

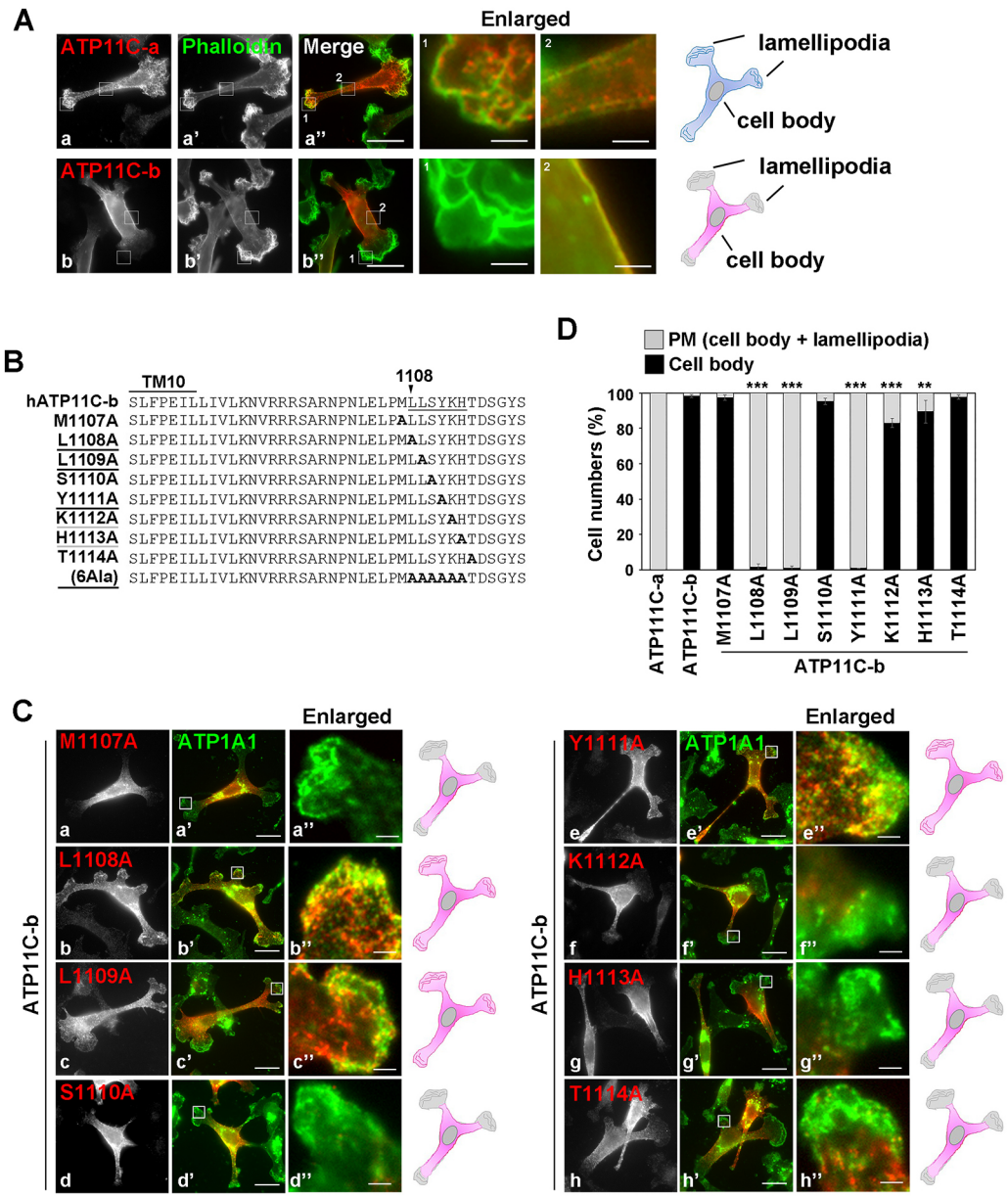

Fig. 6. The LLSYKH residues in C-terminus of ATP11C-b are indispensable for polarized localization. (A) MDA-MB-231 cells, transiently expressing C-terminally HA-tagged ATP11C-a or ATP11C-b and N-terminally FLAG-tagged CDC50A, were fixed and stained for HA and then incubated with Cy3-conjugated anti-rat-IgG antibodies and Alexa Flour 488-conjugated phalloidin. Panels on the right are enlargements of the indicated regions (1, lamellipodia; 2, cell body). Scale bars: 20 µm (main images), 2 µm (enlargements). Illustration shows the schematic localization of ATP11C-a in blue and ATP11C-b in pink. (B) Amino acid sequences of the C-terminal cytoplasmic region of human ATP11C-b and ATP11C-b mutants. Replacement of single amino acid with alanine and that of LLSYKH with six alanine residues are shown. Black underlined mutations eliminated, and gray underlined mutations marginally affected polarized localization of the protein. (C) MDA-MB-231 cells transiently expressing each mutant of ATP11C-b and CDC50A were fixed and stained for HA and ATP1A1 followed by incubation with Cy3-conjugated anti-rat-IgG antibodies and Alexa Fluor 488-conjugated anti-rabbit-IgG secondary antibodies. The illustration shows schematic localization of each mutant of ATP11C-b. (D) Cells expressing ATP11C-a, ATP11C-b and each mutant of ATP11C-b were counted and grouped into two categories: (1) the ATP11C protein localized to the entire plasma membrane, including the cell body and the peripheral lamellipodia (PM); and (2) the ATP11C protein localized to the cell body only but was excluded from the lamellipodia (cell body). Counts were normalized against the total number of cells counted. In each sample, 106–161 cells were counted. Graphs display means±s.d. from three independent experiments. $^{**}P<0.01$, $^{***}P<0.0001$ (one-way ANOVA was performed to assess variance, and comparisons to wild-type of ATP11C-b expressing cells were made using Tukey's post hoc analysis). Scale bars: 20 µm.

Fig. 7D, flippase activity of Ba/F3 cells expressing the ATP11C-b(6Ala) mutant toward PS and PE was comparable to those expressing ATP11C-b(WT). Thus, mislocalization of ATP11C-b was not associated with a change in its enzymatic activity.

We then asked whether ATP11C is required for cell polarity. To this end, we knocked out *Atp11c* using the CRISPR/Cas9 system in Ba/F3 cells (Fig. S6). Three cloned knockout (KO) cell lines (#1-4, #1-5 and #1-6) lost the ability to flip NBD–PS and had a decrease activity for flipping NBD–PE by ∼40% (Fig. 7E), indicating that ATP11C is a major PS-flippase in Ba/F3 cells and it partly contributes to PE-flipping at the plasma membrane. On the other hand, the PC flipping activity was not altered in the *Atp11c*-KO cells. As shown in Fig. 7F, cell polarity was largely unaffected in the *Atp11c*-KO cells; as compared with the parental polarized Ba/F3

Journal of Cell Science (2019) 132, jcs231720. doi:10.1242/jcs.231720

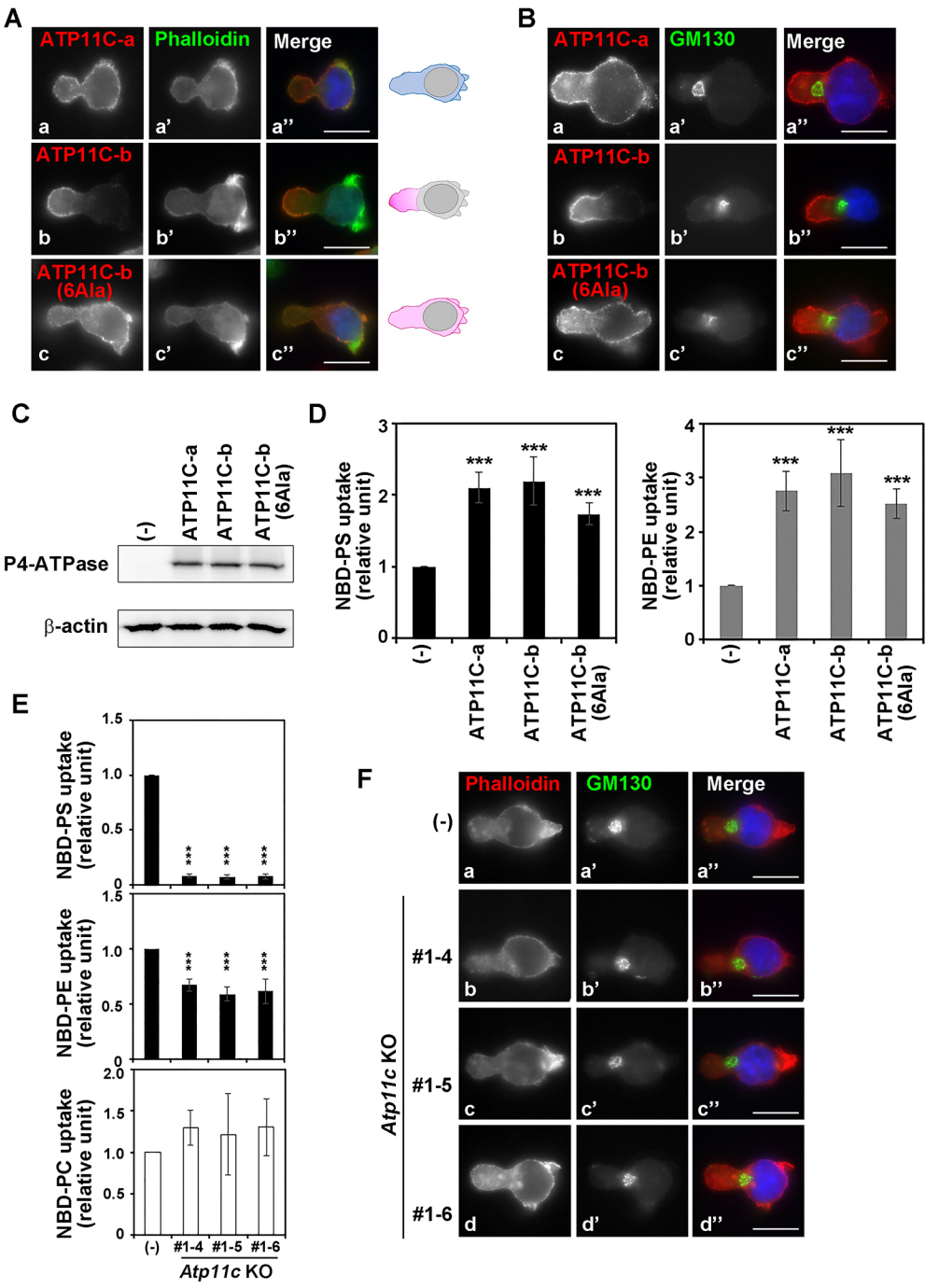

Fig. 7. Loss of the polarized localization of ATP11C-b did not affect cell polarity or flippase activity. (A,B) Ba/F3 cells stably expressing C-terminally HA-tagged ATP11C-a, ATP11C-b or ATP11C-b(6Ala) were stained for HA alone or HA and GM130 followed by Cy3-conjugated anti-rat-IgG antibodies alone or with Alexa Fluor 488-conjugated anti-mouse-IgG secondary antibodies. Alexa Fluor 488-conjugated phalloidin and DAPI were added with the secondary antibodies. Scale bars: 10 µm. The illustration shows the schematic localization of ATP11C-a in blue and ATP11C-b in pink. (C) Ba/F3 cells stably expressing wild-type ATP11C-a or ATP11C-b, or ATP11C-b(6Ala), and parental cells (–) were lysed and subjected to immunoblotting using anti-HA or anti-actin (as an internal control) antibodies. (D,E) Parental Ba/F3 cells (–), and cells stably expressing HA-tagged ATP11C-a, ATP11C-b or ATP11C-b(6Ala) (D), or *Atp11c*-knockout cells (E) were washed with flippase assay buffer and incubated with NBD-PS for 5 min, NBD-PE for 15 min or NBD-PC for 15 min at 15°C. After extraction with fatty acid-free BSA, the residual fluorescence intensity associated with the cells was determined via flow cytometry. The fold increase of NBD lipids uptake is shown relative to that in parental Ba/F3 cells (–). Graph displays means±s.d. from five independent experiments. ***P<0.0001 (one-way ANOVA was performed to assess variance, and comparisons with parental Ba/F3 cells were made using Tukey's post hoc analysis). (F) Parental Ba/F3 cells and *Atp11c*-knockout cells were stained for GM130 followed by Alexa Fluor 488-conjugated anti-mouse-IgG antibodies. Alexa Fluor 555-conjugated phalloidin and DAPI were added with the secondary antibodies. Scale bars: 10 µm.

cells [Fig. 7F(-)], pseudopods and the uropod formed normally (Fig. 7F; Movie 4), and the nucleus and the Golgi complex were located in the normal position. Thus, the polarized localization of ATP11C-b may not be necessary for at least the formation of the anterior–posterior cell polarity.

The LLXYKH residues are sufficient for polarized localization

We next asked whether the LLSYKH residues in the ATP11C-b C-terminal region are sufficient for polarized localization. To this end, we appended the LLSYKH sequence to the C-terminus of ATP11C-a (Fig. 8A) and co-expressed the chimeric protein with FLAG–CDC50A in MDA-MB-231 cells (Fig. 8C). Unlike wild-type ATP11C-a, the ATP11C-a chimera localized exclusively to the cell body and was excluded from the lamellipodia (Fig. 8Ca,b). This observation suggests that the LLXYKH sequence is a sufficient signal for polarized localization. In addition, formation of the lamellipodia was not significantly affected in MDA-MB-231 cells expressing the ATP11C-a chimera (Fig. 8Cb′) as well as in those expressing ATP11C-b(6Ala) (Fig. 8Bb′), suggesting that mislocated ATP11C proteins do not affect lamellipodia formation.

DISCUSSION

In the present study, we investigated the expression levels of C-terminal splice variants of ATP11C in various cell types and tissues, and obtained a comprehensive understanding of their expression profile. Notably, mouse ATP11C-c was predominantly expressed in the brain, although it was marginally expressed in other tissues and most cell types examined in this study. Therefore,

Journal of Cell Science (2019) 132, jcs231720. doi:10.1242/jcs.231720

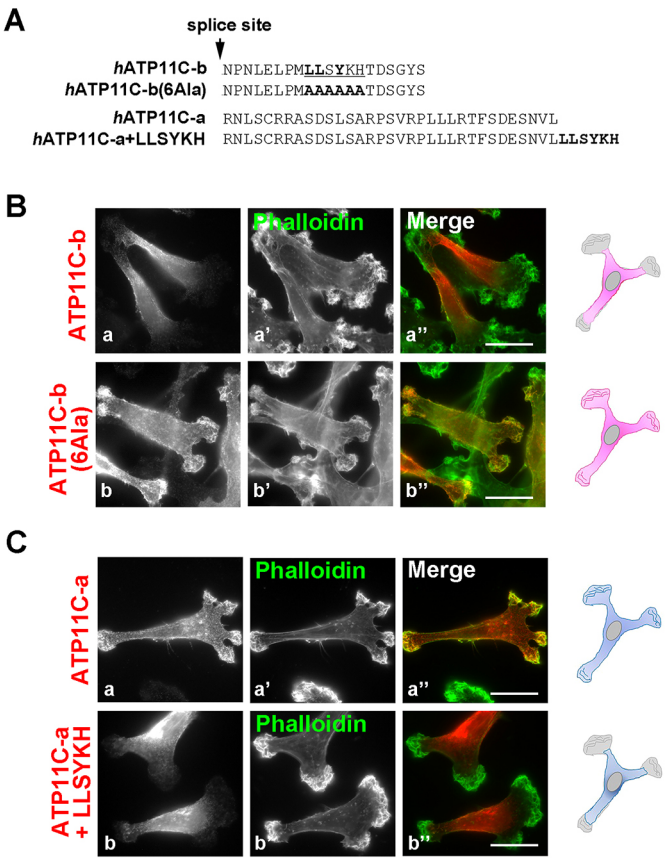

Fig. 8. The LLSYKH residues are sufficient for polarized localization. (A) Amino acid sequences in the C-terminal cytoplasmic region of human ATP11C-b and replacement of LLSYKH with six alanine residues, and ATP11C-a and ATP11C-a chimeric mutants. (B) MDA-MB-231 cells stably expressing ATP11C-b or ATP11C-b(6Ala) were stained for HA, followed by Cy3-conjugated anti-rat-IgG antibody and Alexa Fluor 488-conjugated phalloidin. (C) MDA-MB-231 cells were transiently transfected with the expression vector for C-terminally HA-tagged ATP11C-a or chimeric mutants (ATP11C-a+LLSYKH) and N-terminally FLAG-tagged CDC50A. Cells were stained for HA, followed by Cy3-conjugated anti-rat-IgG antibodies. Alexa Fluor 488-conjugated phalloidin was added with the secondary antibodies. Scale bars: 20 µm.

elucidating the specific roles of ATP11C-a and ATP11C-b in different cell types and those of ATP11C-c in the brain is an important topic for future studies.

We had previously shown that internalization of ATP11C-a is induced by Ca^{2+}-dependent PKCα activation (Takatsu et al., 2017). By contrast, ATP11C-b and ATP11C-c do not undergo endocytosis upon PMA treatment. Therefore, downregulation of ATP11C-a is expected to be critical for cells with predominant expression of this ATP11C variant, and/or for certain membrane domains, such as the lamellipodia and pseudopods, in which ATP11C-b is absent. Chemotactic signals increase the local Ca^{2+} concentration in the cytosol, and this increase is involved in cell migration (Merritt et al., 1991; Negulescu et al., 1996; Wang et al., 2017b). The ATP11C-a variant can be downregulated by a local increase in cytosolic Ca^{2+} concentration (Takatsu et al., 2017), probably resulting in transient PS exposure. Because the transduction of extracellular chemotactic signal and dynamic actin rearrangement take place at the pseudopods and lamellipodia, transbilayer movement of PS through the regulation of the PS-flippase ATP11C-a is possibly important for plasma membrane dynamics. The dynamic transbilayer rearrangement (oscillation) of PS distribution is also likely to contribute to cell polarity. In budding yeast, PS accumulates at the budding and mating sites, and cell polarity requires appropriate Cdc42 recycling (association and dissociation) at the plasma membrane. In addition, the C-terminal cationic region of Cdc42 can interact with anionic phospholipids, such as PS. Indeed, proper activation and recruitment of Cdc42 to the plasma membrane requires the oscillation of local PS concentration, which can be regulated by PE-flippase activity; that is, an increase in PE-flipping activity decreases the local PS concentration on the plasma membrane (Das et al., 2012; Saito et al., 2007). Similarly, ATP8B1 is required for the polarized localization of Cdc42 in mammalian cells (Bruurs et al., 2015). Because ATP8B1 is a PC flippase (Takatsu et al., 2014), the oscillation of local PS concentration can be regulated by PC-flippase activity of ATP8B1 to allow the proper activation and local clustering of Cdc42 at the apical membranes (Bruurs et al., 2015).

Although the physiological roles of ATP11C isoforms are unknown, at least ATP11C isoforms seem to be dispensable for the formation of cell polarity (Fig. 7F; Movie 4). However, we cannot exclude the possibility that they play a role in fine-tuning of cell migration. Because the overexpression of ATP11A and CDC50A increases tumor cell migration (Wang et al., 2017a), and depletion of either ATP8A1 or CDC50A causes a defect in the formation of membrane ruffles and inhibits cell migration, phospholipid flipping activity may play an important role in cell migration (Kato et al., 2013). Although the mechanism by which P4-ATPases are implicated in cell migration is currently unknown, the flipping activity itself is involved in membrane dynamics (Takada et al., 2018; Takeda et al., 2014; Wehman et al., 2011). Given that an increase in PC-flipping activity changes cell shape, attenuates cell adhesion and cell spreading, and drives inward membrane curvature (Miyano et al., 2016; Naito et al., 2015; Takada et al., 2018), transbilayer oscillation of phospholipid distribution would be expected to contribute to membrane dynamics during cell migration. Since ATP11C-b was expressed in invasive breast cancer cells (MDA-MB-231), but not in non-invasive ones (MCF7 and MDA-MB-453) (Thompson et al., 1992; Zajchowski et al., 2001), ATP11C-b is expected to be involved in cell migration. Because ATP11C-b remains localized to the uropod in B cells and the cell body in MDA-MB-231 cells, it is tempting to speculate that transbilayer PS movement would be active at the cell anterior or lamellipodia where ATP11C-a is localized, whereas PS enrichment in the inner leaflet is tightly preserved at the cell posterior or cell body where ATP11C-b is localized. In migrating leukocytes, actin stability is also polarized, with dynamically rearranging F-actin concentrated in leading-edge pseudopods and relatively stable F-actin concentrated at the posterior, where high actomyosin contractility is generated (Hind et al., 2016). ATP11C-b is localized to the adjacent stable actin filaments (Fig. 6A) and, thus, is predicted to play a role in contractile force generation at the cell posterior or cell body during cell migration.

Notably, ATP11C-b appeared to be predominantly expressed in leukocytes (KBM7, Raw264.7, Ba/F3 and W3 cells), spleen and bone marrow, suggesting that ATP11C-b play a role in myeloid and lymphoid cells. ATP11C is expressed and facilitates phospholipid flipping in all leukocytes (Yabas et al., 2016), and CDC50A plays critical roles in hematopoietic cell survival (Li et al., 2018). Moreover, *Atp11c*-deficient mice exhibit a defect in B-cell development and abnormal erythrocyte shape and suffer from anemia (Siggs et al., 2011a; Yabas et al., 2014, 2011), suggesting that these phenotypes may be attributed to a defective mouse ATP11C-b isoform.

Journal of Cell Science (2019) 132, jcs231720. doi:10.1242/jcs.231720

ATP11C is highly expressed in the liver (Chaubey et al., 2016), and its deficiency causes hyperbilirubinemia and hypercholanemia in mice (Siggs et al., 2011b). Moreover, ATP11C appears to be involved in the transport of bile acids across the sinusoidal membrane (de Waart et al., 2016; Matsuzaka et al., 2015). Importantly, we showed that ATP11C-a and ATP11C-b are highly expressed in the liver (Fig. S2). Considering that ATP11C-b was specifically localized to the bile canalicular plasma membrane (apical membrane) in polarized HepG2 cells, we speculate that the two isoforms (ATP11C-a and ATP11C-b) regulate phospholipid asymmetry at distinct areas such as the apical and basolateral plasma membrane in hepatocytes, allowing for the association and/or physiological function of membrane proteins in the polarized plasma membrane (de Waart et al., 2016).

Importantly, the LLSYKH residues appeared to be sufficient for polarized localization of ATP11C-b. Therefore, the LLSYKH residues would be expected to interact with certain proteins or membrane lipids; thus, ATP11C-b can be trapped at the polarized plasma membrane. Searching for binding partners for LLSYKH residues is critical for elucidating the function of ATP11C-b in polarized cells. Considering that replacing single amino acids (L1108, L1109 or Y1111) of ATP11C-b dramatically impairs its polarized localization in MDA-MB-231 cells, but only marginally in Ba/F3 cells, the mechanism for the polarized localization may be subtly different between cell types. Our findings provide insight into physiological roles of ATP11C isoforms, not only in distinct tissues, but also in polarized plasma membrane domains, such as apical and basal, anterior and posterior, or ruffled and unruffled plasma membrane, in conjunction with phenotypes caused by ATP11C deficiency.

MATERIALS AND METHODS

Plasmids

Expression vectors for C-terminally HA-tagged human P4-ATPases were constructed as previously described (Takatsu et al., 2011, 2014). The C-termini of ATP11C-b and ATP11C-c were cloned via RT-PCR from the total RNA of HeLa cells and 293T cells, respectively. Each C-terminus fragment was replaced with C-terminus of ATP11C-a using the In-Fusion HD cloning kit (Clontech) and/or the SLiCE cloning method (Zhang et al., 2012). An expression vector for N-terminally EGFP- or tRFP-tagged ATP11C was constructed by subcloning a cDNA fragment containing the entire coding sequence of human ATP11C-a or ATP11C-b into pMXs-neo-EGFP or pMXs-puro-tRFP. To construct pMXs-neo-EGFP or pMXs-puro-tRFP, DNA fragments encoding EGFP or tRFP were amplified from pEGFP-C1 or pTagRFP-T-C1 (a gift from Hideki Shibata, Nagoya University, Japan) and inserted into the pMXs-neo or pMXs-puro vector, respectively. To construct the amino acid replacement ATP11C-b mutants, each mutation was introduced into the ATP11C-b cDNA via PCR-based, site-directed mutagenesis using the QuikChange II XL site-directed mutagenesis kit (Agilent Technologies) and/or the SLiCE cloning method (Zhang et al., 2012). To construct ATP11C-b(6Ala), and ATP11C-a(+LLSYKH), DNA fragments encoding the C-terminal region of ATP11C with the indicated mutations (base pairs) were synthesized and inserted to replace the same region of wild-type ATP11C cDNA using the SLiCE cloning method (Zhang et al., 2012).

Antibodies and reagents

Sources of antibodies used in the present study were as follows: monoclonal rabbit anti-ATP1A1 (EP1845Y), and monoclonal rat anti-CD44 (1M7.8.1), Abcam; monoclonal mouse anti-HA (4B2), Wako; monoclonal mouse anti-GM130, BD Biosciences; monoclonal mouse anti-β-tubulin (KMX-1), Millipore; monoclonal mouse anti-β-actin (C4), Santa Cruz Biotechnology; monoclonal rat anti-HA (3F10), Roche Applied Science; Alexa Fluor-conjugated secondary antibodies, Invitrogen; Cy3-, DyLight649- and horseradish peroxidase-conjugated secondary antibodies, Jackson ImmunoResearch Laboratories. Dilutions at which primary antibodies were used are provided in Table S1. Dilutions at which primary antibodies were used are provided in Table S1. DAPI and Alexa Fluor 488-conjugated phalloidin were purchased from Molecular Probes.

The NBD-labeled phospholipids (Avanti Polar Lipids) used were: NBD-PS, 1-oleyl-2-[6-[(7-nitro-2-1,3-benzoxadiazol-4-yl)amino]hexanoyl]-sn-glycero-3-phosphoserine; NBD-PE, 1-oleyl-2-[6-[(7-nitro-2-1,3-benzoxadiazol-4-yl)amino]hexanoyl]-sn-glycero-3-phosphoethanolamine; and NBD-PC, 1-oleyl-2-[6-[(7-nitro-2-1,3-benzoxadiazol-4-yl)amino]hexanoyl]-sn-glycero-3-phosphocholine. Phorbol-12-myristate-13-acetate (PMA) was purchased from LC Laboratories.

Cell culture and establishment of stable cell lines

KBM-7 (a gift from Brent Cochran, Tufts University, MA), Raw264.7 (Toshiki Itoh, Kobe University, Japan), BON (gift from Thomas Seufferlein, Ulm University, Germany), Ba/F3 and W3 (gifts from Shigekazu Nagata, Osaka University, Japan), UV-B6, Huh-7, HepG2, and MDA-MB-453 (RIKEN BRC), HUVEC (Lonza), HCT-116 (ATCC), MDA-MB-231, MCF-7 and 3T3-L1 were cultured as described in instruction manuals. The cells expressing recombinant mouse interleukin-3 (IL-3) were kind gifts from Shigekazu Nagata (Osaka University, Japan). Briefly, the IL-3-dependent pro-B-cell line Ba/F3 was maintained in RPMI-1640 medium containing 10% fetal calf serum (Gibco) (Fukunaga et al., 1990). MDA-MB-231 cells were cultured in Dulbecco's modified Eagle's medium (Nacalai Tesque) supplemented with 10% fetal calf serum (Gibco). HepG2 cells were cultured in Dulbecco's modified Eagle's medium (Nacalai Tesque) supplemented with 10% fetal calf serum, GlutaMAX-1 (Gibco) and non-essential amino acids (Nacalai Tesque). HeLa cells were cultured as described previously (Takatsu et al., 2011). Ba/F3, MDA-MB-231, HepG2 cells stably expressing each C-terminally HA-tagged P4-ATPase, C-terminally HA-tagged amino acid mutant ATP11C or N-terminally EGFP-tagged ATP11C were established as described previously (Takatsu et al., 2014). To transiently express P4-ATPases, MDA-MB-231 cells were transfected with a pCAG-HA-based vector carrying P4-ATPase cDNA (C-terminally HA-tagged) and a pcDNA3-FLAG-based vector containing CDC50A cDNA (Takatsu et al., 2011). Transfections were performed via lipofection using Lipofectamine 2000 (Invitrogen). After 1–2 days, the transfected cells were fixed for immunofluorescence analysis. To establish Ba/F3 cells co-expressing EGFP-tagged ATP11C-a and tRFP-tagged ATP11C-b, recombinant retrovirus for expression of tRFP-tagged ATP11C-b was produced and used to infect EGFP-ATP11C-a-expressing Ba/F3 cells. The infected cells were selected in medium containing puromycin (1 µg/ml). A mixed population of drug-resistant cells was used for time-lapse imaging analysis.

Immunofluorescence analysis and time-lapse imaging analysis

Immunostaining was performed as previously described (Shin et al., 2005; Wojtal et al., 2006) and visualized using an Axiovert 200MAT microscope (Carl Zeiss) and an A1R-MP confocal laser-scanning microscope (Nikon). To preserve the polarity of Ba/F3 cells, 3% PFA was added directly to the cultured cells and incubated at room temperature for 30 min. HeLa and MDA-MB-231 cells seeded onto coverslips were fixed with 3% PFA. HepG2 cells seeded onto coverslips, cultured for more than 3 days and fixed with 3% PFA. Cells were then permeabilized with 0.2% saponin for 20 min or 0.1% Triton X-100 for 5 min at room temperature. For time-lapse recording, EGFP–ATP11C-a or EGFP–ATP11C-b and/or tRFP–ATP11C-b-expressing Ba/F3 cells or MDA-MB-231 cells were placed on a microscope stage pre-warmed to 37°C and then observed on an A1R-MP confocal microscope. Images were acquired every 20 s in the presence of 0.5 µg/ml of the nuclear stain Hoechst 33342 (Molecular Probes) and movies play at a rate of 10 frames per second.

RT-PCR and quantitative RT-PCR

Total RNA was extracted from cells and mouse (C57BL/6N) tissues using the RNeasy kit (Qiagen) or Isogen (TOYOBO) and subjected to RT-PCR analysis using the SuperScript III One-Step RT-PCR system (Invitrogen). Fragments of the C-terminus variants of ATP11C were amplified the following primer pairs: for human, forward, 5′-CTGTCTTCTGTATCCAC-ATGGTTG-3′, reverse, 5′-GGCTACTTACAATAATGGTAAATGC-3′; for mouse, forward, 5′-CTTTTCCCTGAGATTCTCCTAATAG-3′, reverse

5′-CTCACTTGGGCCATAATGGCTAC-3′. Fragments of β-actin were amplified the following primer pairs: for human, forward, 5′-GCAAGAG-AGGCATCCTCACC-3′, reverse, 5′-CGTAGATGGGCACAGTGTGG-3′; for mouse, forward, 5′-GCACCACACCTTCTACAATGAG-3′, reverse, 5′-CGTAGATGGGCACAGTGTGG-3′. For quantitative RT-PCR, total RNA was subjected to reverse transcription using ReverTra Ace qPCR RT Master Mix (TOYOBO). The resultant cDNA was used as a template for PCR using THUNDERBIRD SYBR qPCR Mix (TOYOBO). Each fragment of isoforms was amplified using the following primers: for human ATP11C-a, forward: 5′-GAAGAAGAAGTGCCAGGAGAAATC-3′, reverse: 5′-GGCTACTTA-CAATAATGGTAAATGC-3′; for human ATP11C-b, forward: 5′-GTAAG-AAGAAGAAGTGCCAGGAAT-3′, reverse: 5′-GGCTACTTACAATAAT-GGTAAATGC-3′; for mouse ATP11C-a, forward: 5′-GAAGAAGAAGT-GCCAGGAGAAATC-3′, reverse: 5′-CTCACTTGGGCCATAATGGCTAC-3′; for mouse ATP11C-b, forward: 5′-GTTCGAAGAAGAAGTGCCAG-GAAT, reverse: 5′-CTCACTTGGGCCATAATGG-CTAC-3′; for mouse ATP11C-c, forward: 5′-CCTCAGGAACATCTGCTATCTTC-3′, reverse: 5′-CTCACTTGGGC-CATAATGGCTAC-3′. A specific primer set for human ATP11C-c was not successfully designed even with a number of attempts.

Surface biotinylation

The cell-surface biotinylation assay was performed as previously described (Shin et al., 2005; Takatsu et al., 2014). Cells were washed three times with chilled PBS containing 0.1 mM $CaCl_2$ and 0.1 mM $MgCl_2$ (PBS++), and then incubated at 4°C for 30 min with 2 mM sulfo-NHS-LC-biotin (Thermo Fisher Scientific) in PBS++. To stop biotinylation, the cells were washed three times with chilled PBS++ containing 100 mM glycine and 0.3% BSA, and then washed twice more with chilled PBS. The cells were then lysed in lysis buffer [20 mM HEPES-KOH pH 7.4 containing 1% NP-40, 150 mM NaCl, and a protease inhibitor mixture (Complete, Roche Applied Science)] for 30 min at 4°C. The lysates were centrifuged at 20,000 ***g*** at 4°C for 20 min in a microcentrifuge to remove cellular debris and insoluble materials. To precipitate the biotinylated proteins, the supernatant was incubated at 4°C for 4 h with streptavidin–agarose beads (Thermo Fisher Scientific) pre-equilibrated with lysis buffer. The protein-bound streptavidin beads were washed three times with lysis buffer, twice with high-salt buffer (20 mM HEPES-KOH pH 7.4, 500 mM NaCl, 1 mM EDTA, 0.5% NP-40), and once with 20 mM HEPES-KOH (pH 7.4). Proteins were eluted from the beads with SDS-PAGE sample buffer, denatured at 37°C for 2 h and subjected to immunoblot analysis.

Flippase assay

NBD-phospholipid incorporation was analyzed using flow cytometry as previously described (Takatsu et al., 2014). In brief, Ba/F3 cells were harvested from suspension culture by centrifugation. Cells (2×10^5 cells per sample) were washed and equilibrated at 15°C for 15 min in 100 µl of Hank's balanced salt solution (pH 7.4) containing 1 g/l glucose (HBSS-glucose). An equal volume of 2 µM NBD-phospholipid in HBSS-glucose was added to the cell suspension and incubated at 15°C. At each time point, 200 µl of the cell suspension was mixed with 200 µl of ice-cold HBSS-glucose containing 5% fatty acid-free BSA (Wako) to extract NBD-lipids incorporated into the exoplasmic leaflet of the plasma membrane, as well as unincorporated lipids. Next, the cells were analyzed with a FACSCalibur (BD Biosciences) to measure the fluorescence of NBD-lipids incorporated and translocated into the cytoplasmic leaflet of the plasma membrane. Graphs for NBD-lipid flippase activities are expressed as mean±s.d. from at least three independent experiments. Statistical significance was determined using a Student's *t*-test.

Gene editing using the CRISPR/Cas9 system

We disrupted the *Atp11c* gene in Ba/F3 cells using the CRISPR/Cas9 system. Target sequences for the *Atp11c* gene were designed using the CRISPR Design Tool from the Zhang lab (http://crispr.mit.edu). Complementary oligonucleotides (5′-CACCGCAATTACACTCATACGTCGG-3′ and 5′-A-AACCCGACGTATGAGTGTAATTGC-3′) were synthesized and introduced into BsmBI-digested vector lentiCRISPRv2 (Addgene #52961). For lentiviral production, the guide RNA sequence including lentiCRISPRv2 vector were co-transfected with psPAX2 (Addgene #12260) and pMD2.G into HEK293T cells. The resultant lentiviruses were concentrated as described previously (Takatsu et al., 2014) and then used to infect Ba/F3 cells. The infected cells were selected in medium containing G418 (1 mg/ml), and clones were isolated by single-cell sorting with a SH800S Cell Sorter (Sony Biotechnology). For confirmation of editing of *Atp11c*, genomic DNA was extracted from individual clones and subjected to PCR with primer set to amplify Atp11c fragments (forward, 5′-GAGACATTTCGAAGAAAAGTGG-3′, reverse, 5′-TTCAGGACCCTTAGCTCTGG-3′). The knockout (KO) was confirmed by direct sequencing of the amplified PCR product using the forward primer. The flippase assay toward NBD-PS was also performed using the KO clones. The *Atp11c* gene is located on the X chromosome and the male *Sry* transcript was detected by RT-PCR in Ba/F3 cells. A single allelic indel at the *Atp11c* locus was observed for seven of 11 KO clones. However, we unexpectedly found that four of the 11 KO clones carried biallelic indels. Although we do not know the exact reason for the biallelic indels, they might be derived from the duplication of the *Atp11c* locus. In this study, we chose two clones with a single allelic indel (#1-4 and #1-5) and a clone with double allelic indels (#1-6) (Fig. S6), all of which were confirmed to lose the PS-flipping activities (Fig. 7E).

Acknowledgements

We thank Shigekazu Nagata, Thomas Seufferlein, Brent Cochran and Toshiki Itoh for kindly providing cell lines, Toshio Kitamura (The University of Tokyo) and Hiroyuki Miyoshi (RIKEN BioResource Center) for providing plasmids for retroviral infection, and Hideki Shibata (Nagoya University) for providing a plasmid. We also thank Shohei Nozaki for technical support of DNA sequencing analysis.

Competing interests

The authors declare no competing or financial interests.

Author contributions

Conceptualization: H.T., H.-W.S.; Methodology: M.T., H.T., T.N., H.-W.S.; Validation: H.T., H.-W.S.; Formal analysis: M.T., H.T., H.I., A.H., T.N., K.N., H.-W.S.; Investigation: M.T., H.T., A.H., H.I.; Resources: M.T., H.T., T.N., H.-W.S.; Data curation: H.T., H.-W.S.; Writing - original draft: H.-W.S.; Writing - review & editing: H.T., T.N., K.N., H.-W.S.; Visualization: M.T., H.T., A.H., H.I., H.-W.S.; Supervision: H.-W.S.; Project administration: H.-W.S.; Funding acquisition: H.T., H.-W.S.

Funding

This work was supported by Japan Society for the Promotion of Science (JSPS) KAKENHI Grant Numbers JP17H03655 (to H.-W.S.) and JP17K08270 (to H.T.); the Takeda Science Foundation (to H.-W.S.); the Japan Foundation for Applied Enzymology (to H.-W.S); and the Naito Foundation (to H.-W.S.).

Supplementary information

Supplementary information available online at
http://jcs.biologists.org/lookup/doi/10.1242/jcs.231720.supplemental

References

Andersen, J. P., Vestergaard, A. L., Mikkelsen, S. A., Mogensen, L. S., Chalat, M. and Molday, R. S. (2016). P4-ATPases as phospholipid flippases-structure, function, and enigmas. *Front. Physiol.* **7**, 275. doi:10.3389/fphys.2016.00275

Arashiki, N., Takakuwa, Y., Mohandas, N., Hale, J., Yoshida, K., Ogura, H., Utsugisawa, T., Ohga, S., Miyano, S., Ogawa, S. et al. (2016). ATP11C is a major flippase in human erythrocytes and its defect causes congenital hemolytic anemia. *Haematologica* **101**, 559-565. doi:10.3324/haematol.2016.142273

Bonifacino, J. S. and Traub, L. M. (2003). Signals for sorting of transmembrane proteins to endosomes and lysosomes. *Annu. Rev. Biochem.* **72**, 395-447. doi:10.1146/annurev.biochem.72.121801.161800

Bruurs, L. J. M., Donker, L., Zwakenberg, S., Zwartkruis, F. J., Begthel, H., Knisely, A. S., Posthuma, G., van de Graaf, S. F. J., Paulusma, C. C. and Bos, J. L. (2015). ATP8B1-mediated spatial organization of Cdc42 signaling maintains singularity during enterocyte polarization. *J. Cell Biol.* **210**, 1055-1063. doi:10.1083/jcb.201505118

Chaubey, P. M., Hofstetter, L., Roschitzki, B. and Stieger, B. (2016). Proteomic analysis of the rat canalicular membrane reveals expression of a complex system of P4-ATPases in liver. *PLoS ONE* **11**, e0158033. doi:10.1371/journal.pone.0158033

Das, A., Slaughter, B. D., Unruh, J. R., Bradford, W. D., Alexander, R., Rubinstein, B. and Li, R. (2012). Flippase-mediated phospholipid asymmetry promotes fast Cdc42 recycling in dynamic maintenance of cell polarity. *Nat. Cell Biol.* **14**, 304-310. doi:10.1038/ncb2444

de Waart, D. R., Naik, J., Utsunomiya, K. S., Duijst, S., Ho-Mok, K., Bolier, A. R., Hiralall, J., Bull, L. N., Bosma, P. J., Oude Elferink, R. P. et al. (2016). ATP11C

targets basolateral bile salt transporter proteins in mouse central hepatocytes. *Hepatology* **64**, 161-174. doi:10.1002/hep.28522
Devaux, P. F. (1991). Static and dynamic lipid asymmetry in cell membranes. *Biochemistry* **30**, 1163-1173. doi:10.1021/bi00219a001
Fairn, G. D., Schieber, N. L., Ariotti, N., Murphy, S., Kuerschner, L., Webb, R. I., Grinstein, S. and Parton, R. G. (2011). High-resolution mapping reveals topologically distinct cellular pools of phosphatidylserine. *J. Cell Biol.* **194**, 257-275. doi:10.1083/jcb.201012028
Finkielstein, C. V., Overduin, M. and Capelluto, D. G. S. (2006). Cell migration and signaling specificity is determined by the phosphatidylserine recognition motif of rac1. *J. Biol. Chem.* **281**, 27317-27326. doi:10.1074/jbc.M605560200
Fukunaga, R., Ishizaka-Ikeda, E. and Nagata, S. (1990). Purification and characterization of the receptor for murine granulocyte colony-stimulating factor. *J. Biol. Chem.* **265**, 14008-14015. doi:10.1016/0092-8674(90)90814-u
Hind, L. E., Vincent, W. J. and Huttenlocher, A. (2016). Leading from the back: the role of the uropod in neutrophil polarization and migration. *Dev. Cell* **38**, 161-169. doi:10.1016/j.devcel.2016.06.031
Kato, U., Inadome, H., Yamamoto, M., Emoto, K., Kobayashi, T. and Umeda, M. (2013). Role for phospholipid flippase complex of ATP8A1 and CDC50A proteins in cell migration. *J. Biol. Chem.* **288**, 4922-4934. doi:10.1074/jbc.M112.402701
Kelly, B. T., McCoy, A. J., Spate, K., Miller, S. E., Evans, P. R., Honing, S. and Owen, D. J. (2008). A structural explanation for the binding of endocytic dileucine motifs by the AP2 complex. *Nature* **456**, 976-979. doi:10.1038/nature07422
Lee, S., Uchida, Y., Wang, J., Matsudaira, T., Nakagawa, T., Kishimoto, T., Mukai, K., Inaba, T., Kobayashi, T., Molday, R. S. et al. (2015). Transport through recycling endosomes requires EHD1 recruitment by a phosphatidylserine translocase. *EMBO J.* **34**, 669-688. doi:10.15252/embj.201489703
Li, N., Yang, Y., Liang, C., Qiu, Q., Pan, C., Li, M., Yang, S., Chen, L., Zhu, X. and Hu, Y. (2018). Tmem30a plays critical roles in ensuring the survival of hematopoietic cells and leukemia cells in mice. *Am. J. Pathol.* **188**, 1457-1468. doi:10.1016/j.ajpath.2018.02.015
Matsuzaka, Y., Hayashi, H. and Kusuhara, H. (2015). Impaired hepatic uptake by organic anion-transporting polypeptides is associated with hyperbilirubinemia and hypercholanemia in Atp11c mutant mice. *Mol. Pharmacol.* **88**, 1085-1092. doi:10.1124/mol.115.100578
Merritt, J. E., Greener, M., Hallam, T. J. and Swayne, G. T. (1991). The involvement of calcium and protein kinase C in modulating agonist-stimulated chemotaxis of human neutrophils. *Cell. Signal.* **3**, 73-77. doi:10.1016/0898-6568(91)90010-R
Miyano, R., Matsumoto, T., Takatsu, H., Nakayama, K. and Shin, H. W. (2016). Alteration of transbilayer phospholipid compositions is involved in cell adhesion, cell spreading, and focal adhesion formation. *FEBS Lett.* **590**, 2138-2145. doi:10.1002/1873-3468.12247
Murate, M., Abe, M., Kasahara, K., Iwabuchi, K., Umeda, M. and Kobayashi, T. (2015). Transbilayer distribution of lipids at nano scale. *J. Cell Sci.* **128**, 1627-1638. doi:10.1242/jcs.163105
Naito, T., Takatsu, H., Miyano, R., Takada, N., Nakayama, K. and Shin, H.-W. (2015). Phospholipid flippase ATP10A translocates phosphatidylcholine and is involved in plasma membrane dynamics. *J. Biol. Chem.* **290**, 15004-15017. doi:10.1074/jbc.M115.655191
Negulescu, P. A., Krasieva, T. B., Khan, A., Kerschbaum, H. H. and Cahalan, M. D. (1996). Polarity of T cell shape, motility, and sensitivity to antigen. *Immunity* **4**, 421-430. doi:10.1016/S1074-7613(00)80409-4
Niggli, V. (2014). Insights into the mechanism for dictating polarity in migrating T-cells. *Int. Rev. Cell Mol. Biol.* **312**, 201-270. doi:10.1016/B978-0-12-800178-3.00007-5
Roland, B. P., Naito, T., Best, J. T., Arnaiz-Yépez, C., Takatsu, H., Yu, R. J., Shin, H. W. and Graham, T. R. (2019). Yeast and human P4-ATPases transport glycosphingolipids using conserved structural motifs. *J. Biol. Chem.* **294**, 1794-1806. doi:10.1074/jbc.RA118.005876
Saito, K., Fujimura-Kamada, K., Hanamatsu, H., Kato, U., Umeda, M., Kozminski, K. G. and Tanaka, K. (2007). Transbilayer phospholipid flipping regulates Cdc42p signaling during polarized cell growth via Rga GTPase-activating proteins. *Dev. Cell* **13**, 743-751. doi:10.1016/j.devcel.2007.09.014
Segawa, K., Kurata, S., Yanagihashi, Y., Brummelkamp, T. R., Matsuda, F. and Nagata, S. (2014). Caspase-mediated cleavage of phospholipid flippase for apoptotic phosphatidylserine exposure. *Science* **344**, 1164-1168. doi:10.1126/science.1252809
Segawa, K., Yanagihashi, Y., Yamada, K., Suzuki, C., Uchiyama, Y. and Nagata, S. (2018). Phospholipid flippases enable precursor B cells to flee engulfment by macrophages. *Proc. Natl. Acad. Sci. USA* **115**, 12212-12217. doi:10.1073/pnas.1814323115
Shin, H. W. and Takatsu, H. (2019). Substrates of P4-ATPases: beyond aminophospholipids (phosphatidylserine and phosphatidylethanolamine). *FASEB J.* **33**, 3087-3096. doi:10.1096/fj.201801873R
Shin, H.-W., Kobayashi, H., Kitamura, M., Waguri, S., Suganuma, T., Uchiyama, Y. and Nakayama, K. (2005). Roles of ARFRP1 (ADP-ribosylation factor-related protein 1) in post-Golgi membrane trafficking. *J. Cell Sci.* **118**, 4039-4048. doi:10.1242/jcs.02524
Siggs, O. M., Arnold, C. N., Huber, C., Pirie, E., Xia, Y., Lin, P., Nemazee, D. and Beutler, B. (2011a). The P4-type ATPase ATP11C is essential for B lymphopoiesis in adult bone marrow. *Nat. Immunol.* **12**, 434-440. doi:10.1038/ni.2012
Siggs, O. M., Schnabl, B., Webb, B. and Beutler, B. (2011b). X-linked cholestasis in mouse due to mutations of the P4-ATPase ATP11C. *Proc. Natl Acad. Sci. USA* **108**, 7890-7895. doi:10.1073/pnas.1104631108
Sormunen, R., Eskelinen, S. and Lehto, V. P. (1993). Bile canaliculus formation in cultured HEPG2 cells. *Lab. Invest.* **68**, 652-662.
Takada, N., Takatsu, H., Miyano, R., Nakayama, K. and Shin, H. W. (2015). ATP11C mutation is responsible for the defect in phosphatidylserine uptake in UPS-1 cells. *J. Lipid Res.* **56**, 2151-2157. doi:10.1194/jlr.M062547
Takada, N., Naito, T., Inoue, T., Nakayama, K., Takatsu, H. and Shin, H. W. (2018). Phospholipid-flipping activity of P4-ATPase drives membrane curvature. *EMBO J.* **37**, e97705. doi:10.15252/embj.201797705
Takatsu, H., Baba, K., Shima, T., Umino, H., Kato, U., Umeda, M., Nakayama, K. and Shin, H.-W. (2011). ATP9B, a P4-ATPase (a Putative Aminophospholipid Translocase), localizes to the trans-golgi network in a CDC50 protein-independent manner. *J. Biol. Chem.* **286**, 38159-38167. doi:10.1074/jbc.M111.281006
Takatsu, H., Tanaka, G., Segawa, K., Suzuki, J., Nagata, S., Nakayama, K. and Shin, H.-W. (2014). Phospholipid flippase activities and substrate specificities of human type IV P-type ATPases localized to the plasma membrane. *J. Biol. Chem.* **289**, 33543-33556. doi:10.1074/jbc.M114.593012
Takatsu, H., Takayama, M., Naito, T., Takada, N., Tsumagari, K., Ishihama, Y., Nakayama, K. and Shin, H. W. (2017). Phospholipid flippase ATP11C is endocytosed and downregulated following Ca2+-mediated protein kinase C activation. *Nat. Commun.* **8**, 1423. doi:10.1038/s41467-017-01338-1
Takeda, M., Yamagami, K. and Tanaka, K. (2014). Role of phosphatidylserine in phospholipid flippase-mediated vesicle transport in Saccharomyces cerevisiae. *Eukaryot. Cell* **13**, 363-375. doi:10.1128/EC.00279-13
Tanaka, Y., Ono, N., Shima, T., Tanaka, G., Katoh, Y., Nakayama, K., Takatsu, H. and Shin, H.-W. (2016). The phospholipid flippase ATP9A is required for recycling pathway from endosomes to the plasma membrane. *Mol. Biol. Cell* **27**, 3883-3893. doi:10.1091/mbc.E16-08-0586
Thompson, E. W., Paik, S., Brünner, N., Sommers, C. L., Zugmaier, G., Clarke, R., Shima, T. B., Torri, J., Donahue, S., Lippman, M. E. et al. (1992). Association of increased basement membrane invasiveness with absence of estrogen receptor and expression of vimentin in human breast cancer cell lines. *J. Cell. Physiol.* **150**, 534-544. doi:10.1002/jcp.1041500314
Uchida, Y., Hasegawa, J., Chinnapen, D., Inoue, T., Okazaki, S., Kato, R., Wakatsuki, S., Misaki, R., Koike, M., Uchiyama, Y. et al. (2011). Intracellular phosphatidylserine is essential for retrograde membrane traffic through endosomes. *Proc. Natl Acad. Sci. USA* **108**, 15846-15851. doi:10.1073/pnas.1109101108
Valignat, M.-P., Nègre, P., Cadra, S., Lellouch, A. C., Gallet, F., Hénon, S. and Theodoly, O. (2014). Lymphocytes can self-steer passively with wind vane uropods. *Nat. Commun.* **5**, 5213. doi:10.1038/ncomms6213
Wang, J., Wang, Q., Lu, D., Zhou, F., Wang, D., Feng, R., Wang, K., Molday, R., Xie, J. and Wen, T. (2017a). A biosystems approach to identify the molecular signaling mechanisms of TMEM30A during tumor migration. *PLoS ONE* **12**, e0179900. doi:10.1371/journal.pone.0179900
Wang, X., Qin, W., Xu, X., Xiong, Y., Zhang, Y., Zhang, H. and Sun, B. (2017b). Endotoxin-induced autocrine ATP signaling inhibits neutrophil chemotaxis through enhancing myosin light chain phosphorylation. *Proc. Natl. Acad. Sci. USA* **114**, 4483-4488. doi:10.1073/pnas.1616752114
Wehman, A. M., Poggioli, C., Schweinsberg, P., Grant, B. D. and Nance, J. (2011). The P4-ATPase TAT-5 inhibits the budding of extracellular vesicles in C. elegans embryos. *Curr. Biol.* **21**, 1951-1959. doi:10.1016/j.cub.2011.10.040
Wojtal, K. A., de Vries, E., Hoekstra, D. and van Ijzendoorn, S. C. (2006). Efficient trafficking of MDR1/P-glycoprotein to apical canalicular plasma membranes in HepG2 cells requires PKA-RIIalpha anchoring and glucosylceramide. *Mol. Biol. Cell* **17**, 3638-3650. doi:10.1091/mbc.e06-03-0230
Yabas, M., Teh, C. E., Frankenreiter, S., Lal, D., Roots, C. M., Whittle, B., Andrews, D. T., Zhang, Y., Teoh, N. C., Sprent, J. et al. (2011). ATP11C is critical for the internalization of phosphatidylserine and differentiation of B lymphocytes. *Nat. Immunol.* **12**, 441-449. doi:10.1038/ni.2011
Yabas, M., Coupland, L. A., Cromer, D., Winterberg, M., Teoh, N. C., D'Rozario, J., Kirk, K., Broer, S., Parish, C. R. and Enders, A. (2014). Mice deficient in the putative phospholipid flippase ATP11C exhibit altered erythrocyte shape, anemia and reduced erythrocyte lifespan. *J. Biol. Chem.* **289**, 19531-19537. doi:10.1074/jbc.C114.570267
Yabas, M., Jing, W., Shafik, S., Bröer, S. and Enders, A. (2016). ATP11C facilitates phospholipid translocation across the plasma membrane of all leukocytes. *PLoS ONE* **11**, e0146774. doi:10.1371/journal.pone.0146774
Yeung, T., Heit, B., Dubuisson, J.-F., Fairn, G. D., Chiu, B., Inman, R., Kapus, A., Swanson, M. and Grinstein, S. (2009). Contribution of phosphatidylserine to membrane surface charge and protein targeting during phagosome maturation. *J. Cell Biol.* **185**, 917-928. doi:10.1083/jcb.200903020

Zachowski, A. (1993). Phospholipids in animal eukaryotic membranes: transverse asymmetry and movement. *Biochem. J.* **294**, 1-14. doi:10.1042/bj2940001

Zajchowski, D. A., Bartholdi, M. F., Gong, Y., Webster, L., Liu, H. L., Munishkin, A., Beauheim, C., Harvey, S., Ethier, S. P. and Johnson, P. H. (2001). Identification of gene expression profiles that predict the aggressive behavior of breast cancer cells. *Cancer Res.* **61**, 5168-5178.

Zegers, M. M. and Hoekstra, D. (1998). Mechanisms and functional features of polarized membrane traffic in epithelial and hepatic cells. *Biochem. J.* **336**, 257-269. doi:10.1042/bj3360257

Zhang, Y., Werling, U. and Edelmann, W. (2012). SLiCE: a novel bacterial cell extract-based DNA cloning method. *Nucleic Acids Res.* **40**, e55. doi:10.1093/nar/gkr1288